Research Article

www.ijrap.net

(ISSN Online:2229–3566, ISSN Print:2277–4343)

FORMULATION, OPTIMISATION AND CHARACTERISATION OF *ARTOCARPUS ALTILIS* LOADED LIPOSOMES FOR ANTIDIABETIC ACTIVITY

Archana M. Patil [1], Sarvanan Kaliyaperumal [2], Mrityunjaya B. Patil [3]*

[1] Department of Pharmacognosy, Maratha Mandal's College of Pharmacy, Belagavi, Karnataka, India

[2] Faculty of Pharmacy, Bhagwant University, Ajmer, Rajasthan, India

[3] Department of Pharmacognosy, KLE College of Pharmacy, Belagavi, KLE Academy of Higher Education and Research, Belagavi, Karnataka, India

Received on: 28/01/23 Accepted on: 22/02/23

***Corresponding author**
E-mail: patil9367@gmail.com

DOI: 10.7897/2277-4343.140248

ABSTRACT

Background: *Artocarpus altilis* primarily comprises phenolic phytoconstituents such as flavonoids, arylbenzofurans, and stilbenoids. This plant has traditionally been known to have glycemic control properties. This study used a design expert approach to create and test *Artocarpus altilis* liposomes for antidiabetic activity. Methods: Design Expert 13 software developed and optimised the liposomal formulation. The optimised formulation was tested for antidiabetic properties in a Streptozotocin-nicotinamide-induced model for 28 days, followed by an oral glucose tolerance test. Biochemical parameters such as lipid profile and glycogen content were also measured at the end of the study. Results: The formation of *Artocarpus altilis* loaded liposomes was confirmed by SEM analysis and entrapment efficiency. Further pharmacology research revealed that *Artocarpus altilis* lowers blood glucose levels by sensitising insulin secretion, maintaining pancreatic beta cell mass, increasing glucose uptake in skeletal muscles, and regulating lipid profiles. Conclusion: The current study reflected the formulation of *Artocarpus altilis* loaded liposomes, its entrapment efficiency, stability study, and its antidiabetic evaluation based on *in vivo* results.

Keywords: *Artocarpus altilis* Liposomes, Quality by Design, Antidiabetic Activity.

INTRODUCTION

Diabetes mellitus (DM) is a chronic metabolic disorder characterised by higher-than-normal blood glucose levels. Diabetes is caused by either the destruction of pancreatic beta cells (Type I), which results in decreased insulin production, or the body tissues' reduced sensitivity to insulin (Type II DM). According to the International Diabetes Federation (IDF) report 2021, 422 million people have diabetes. Diabetes is expected to affect 643 million adults by 2030. Diabetes, along with endocrine and metabolic diseases, will become a global pandemic, according to epidemiological studies. The vast majority of diabetics have type 2 diabetes mellitus, which causes insulin secretion and insulin resistance issues. Moderate exercise, hypoglycemic, dietary control, and lipid-lowering medications are the most commonly used treatments for Type 2 diabetes mellitus. [1-4]

The traditional tree known as breadfruit is *Artocarpus altilis*, which belongs to the Moraceae family. It is native to New Guinea and is widely cultivated in southern India. The tree stands 15-30 meters tall. Breadfruit is an agroforestry tree crop grown primarily for its nutritious, starchy fruit high in carbohydrates, calcium, and phosphorus. The large, thick, leathery leaves are deeply cut into pinnate lobes and have a dark-green, glossy dorsal side. The leaves appear as clusters of varying size and shape at the branches' tips. When the trees are young or grown in the shade, their crowns are conical; as they age, the crowns become rounded and irregular. The blade is smooth and glossy, with green or yellow-green veins and a dense network of white to reddish-white hairs on the midrib and vein. Phytocompounds are biologically active secondary metabolites derived from plants. Morin, ursolic acid, dihydromorin, cynomacurin, betullic acid acetate, artocarpin, oxydihydroartocarpesin, isoartocarpin, cyloartocarpin, artocarpetin, norartocarpetin, cycloartinone, -sitosterol, and artocarpanone are phytocompounds found in the leaves. [5-8]

Liposomes have evolved as a useful tool for studying the function of cell membranes' function and as novel drug carriers with benefits such as improved efficacy and lower toxicity. Liposomes are currently one of the most effective novel drug delivery systems due to their ability to encapsulate various drug entities, which improves biocompatibility and allows for simple interaction with bio-membranes. [9, 10]

Liposome formulations not only improve or alter drug uptake and release but also protect sensitive active agents from degradation in the gastrointestinal tract, reduce gastrointestinal side effects, and even mask the bitter taste of orally administered drugs. [11]

Thus, the current study aimed to prepare, optimise, and evaluate *Artocarpus altilis* loaded liposomes for antidiabetic activity using 3^2 factorial designs. The liposomes were created using the thin film hydration method and then optimised and characterised. The optimised liposomal formulation was also tested for antidiabetic activity and short-term stability.

MATERIALS AND METHODS

Artocarpus altilis leaves were collected in the Chorla region of Goa, India. The leaves were authenticated at the Raja Lakhamagouda Science Institute of the KLE Society on College Road in Belagavi. Lipoid, Germany, provided Phospholipid 90G

as a gift sample. Sigma Life Science in Bangalore, India, provided the cholesterol.

Preparation Method-*Artocarpus altilis* loaded liposomes (AA-LPs)

The thin film hydration method was used to create liposomes. In a round bottom flask, 20ml of chloroform: methanol (2:1) was used to dissolve the drug (*Artocarpus altilis* extract), phospholipid, and cholesterol. A rotary evaporator was used to evaporate the solvent at 60 °C for 1 hour at 70-100 rpm. A thin film was formed on the walls of a round bottom flask, which was then dried overnight in a desiccator to remove any remaining solvent. This thin film was hydrated for 1 hour at 70-100 rpm in 20 ml phosphate buffer pH 7.4 at 60 °C. Overnight, the suspension is allowed to swell to form multilamellar vesicles (MLV) of liposomes. The suspension was then sonicated with a probe sonicator to reduce the size of the vesicles from MLV to small unilamellar vesicles (SUV). Liposomes were kept at 4 °C in an airtight container [12].

Characterisation of *Artocarpus altilis* loaded liposomes (AA-LPs)

Vesicle size and PDI
The Zetasizer Nano ZS was used to determine vesicle size and polydispersity index (PDI) (Malvern Instruments Ltd., Malvern, UK). 20 ml milli-Q water was mixed with 1 ml AA-LP. [13].

Entrapment efficiency
The ultracentrifuge was used to determine the efficiency of entrapment. 1ml of *Artocarpus altilis* loaded liposomes were placed in an Eppendorf tube and centrifuged for 3 hours at 20,000 rpm at 4 ºC. The free drug supernatant was separated and analysed at max260 nm with a UV-Visible spectrophotometer. [14] Entrapment efficiency was calculated as follows:

$$EE\% = \frac{total\ drug - free\ drug\ in\ supernatant}{total\ drug}$$

Scanning Electron Microscopy
SEM-Scanning Electron Microscopy characterised the AA-LPs (S 3400N, Hitachi, Japan). It is used to investigate the shape and surface morphology of AA-LP formulations that have been optimised. A scanning electron microscope examined one drop of liposome suspension on a clean glass slab. [15]

Experimental design
The liposomal formulation was created and optimised using a 32-factorial design. The responses were evaluated using two factors with three different levels. Liposomes' independent variables were the amount of phospholipid and the amount of cholesterol, while the dependent variables were vesicle size (nm) and entrapment efficiency (%). Using DesignExpert® software, combinations of nine batches were run for experimental trials (Version 13.0, Stat-Ease Inc., Minneapolis, MN, USA). The amount of drug (AA) used in each batch of liposomes was kept constant (80 mg). [16-18]

***In vitro* dissolution studies**
The drug was released using a modified dissolution apparatus XXI. *Artocarpus altilis* plain drug solution, Liposomal formulation of *Artocarpus altilis* (AA-LP), and glibenclamide were used as standards. It comprises a 250 ml beaker and a plastic tube with a diameter of 17.5mm that is open on both ends. One end of the tube was tied with a cellophane membrane and dipped into a beaker containing phosphate buffer pH 7.4 dissolution medium, where the temperature was kept constant at 37 °C 0.5, and the speed was kept constant at 100 rpm. A sample of 10 ml optimised liposomes, plain extract solution, and the standard formulation was added to the different tubes, and a paddle stirrer was attached to the beaker's centre. 5 ml samples were taken at 0.5, 1, 2, 4, 6, 8, 10, 12, and 24 hours and spectrophotometrically analysed. [19, 20]

Stability studies
For 6 months, AA-LPs were tested for stability using ICH guidelines at three different temperatures: 4 2 °C, 25 2 °C, and 40 2 °C. It was evaluated for vesicle size and entrapment efficiency at definite time intervals of 0, 2, 4, and 6 months. [21]

Experimental pharmacology (animal study)

Animals Procurement and ethical clearance
The Institutional Animal Ethics Committee of Maratha Mandal's College of Pharmacy, Belagavi, approved the use of animals (Albino Wistar rats). MMCP/2016-17/B.Ph/17414 is the reference number. The animals were purchased from a supplier approved by the committee to control and supervise experimental animals, and they were kept in a pathogen-free environment. Wistar rats of both sexes were used in the study. The average animal weight was (187.36.76) g.

Diabetes induction and animal grouping
Masiello *et al*. described using streptozotocin and nicotinamide to induce diabetes with minor modifications. Nicotinamide (230 mg/kg) was given 15 minutes before the intraperitoneal injection of streptozotocin (65 mg/kg). To prepare fresh injection solutions, the reagents were dissolved in cold citrate buffer (pH 4.5) and water. 2 Animals with fasting blood glucose levels greater than 250 mg/kg were included in the study after 7 days of injection. The animals were divided into five groups, each with six animals (n=6 per group). [22]

In total, 30 animals were used, with 24 successfully induced diabetes mellitus and 6 serving as the standard control group. In the vehicle, AAL and Glibenclamide (GLB) were suspended. Normal: vehicle-treated (Group 1). Diabetic: vehicle-treated (Group 2). (Group 3) Diabetic receiving GLB treatment. Diabetic (Group 4): AAE-400 treatment. Diabetic (Group 5): AAL-400 treatment. The doses were chosen based on previously published doses, optimised formulations, and *in vitro* results.

Measurements and methods

Body weight measurements were taken on the 1st, 7th, 14th, 21st and 28th day following treatment.
The oral glucose tolerance test (OGTT), which measures blood glucose, was performed on the animals after 28 days of therapy while they were fasting (glucometer).[23] Serum analysis was performed after the study, and blood samples were drawn using the cardiac puncture method. The serum was separated by centrifugation for 20 minutes at 4000-5000 rpm. The supernatant was used to estimate the lipid profile, which included total cholesterol (TC), triglycerides (TG), and high-density lipoprotein (HDL), using Agappe Diagnostics LTD's MISPA NANO PLUS automated biochemistry analyser. The levels of low-density lipoprotein (LDL) and very-low-density lipoprotein (VLDL) were calculated using the following equations: LDL (mg/dL) equals TC - (HDL + VLDL), and VLDL (mg/dL) equals TG/5. The ability of the rat hemi diaphragm to absorb glucose and the amount of glycogen in the liver and skeletal muscle were also assessed after 28 days of therapy. Before individual studies, the organs were thoroughly cleaned in cold phosphate buffer to remove blood clots.

The method used to calculate the percentage of glucose uptake in the rat hemi diaphragm was slightly modified from that described by Kumar *et al*. [23]. In a nutshell, an isolated rat hemi diaphragm (10 mm) was incubated for 30 minutes in glucose solution (30 mmol/L, premixed with 0.25 U of insulin) while being aerated with 30 bubbles per minute. Glucose uptake (%) = (Ac - At)/Ac 100, where Ac and At represent the absorbance of the rat hemi diaphragm before and after incubation in a glucose solution, respectively, was calculated as the difference between the initial and final glucose content in the incubation medium using the following formula.

The anthrone method calculated glycogen concentrations in the liver and skeletal muscle [24]. The homogenate was heated briefly in a boiling water bath for 20 minutes while incubating with KOH (30%, 2 mL), then cooled and centrifuged for 15 minutes. To obtain a supernatant volume of up to 25 mL, KOH (30%) was used. Glycogen was precipitated from this solution by adding 95% ethanol (10 mL) and leaving it at room temperature overnight. The entire mixture was then centrifuged at 3000 rpm for 15 minutes. The pellet was dissolved in 1 mL of water, followed by 4 mL of anthrone reagent, and the mixture was heated in a water bath for 10 minutes. After cooling the mixture, the absorbance at 620 nm was measured with an ultraviolet (UV) spectrophotometer (Shimadzu, UVProbe 2.4.3).

Statistical analysis

All experimental results were presented using the mean standard error of the mean. The one-way analysis of variance was performed using Graph Pad Prism, followed by the posthoc Tukey's test as needed (Version 8; GraphPad Software Corporation, San Diego, California, USA).

Table 1

Formulations	Extract (mg)	Phospholipon 90G (mg)	Cholesterol (mg)	PBS pH 7.4 (ml)	Particle size (nm)	EE%
AA-LP 1	80	750	50	20	73.25	72.3
AA-LP 2	80	750	150	20	62.31	79.4
AA-LP 3	80	750	250	20	57.11	77.1
AA-LP 4	80	850	50	20	123.5	76.2
AA-LP 5	80	850	150	20	147.6	81.3
AA-LP 6	80	850	250	20	124.8	78.8
AA-LP 7	80	950	50	20	252.4	77.6
AA-LP 8	80	950	150	20	207.9	82.7
AA-LP 9	80	950	250	20	184.5	79.2

Table 2 Summary of statistical parameters – analysis of variance test (ANOVA)

Response	SS	DF	MS	F-value	P-value	R^2	Adjusted R^2	Model significance
Y_1	34234.16	2	17117.08	36.23	0.0004	0.9235	0.8980	Significant
Y_2	49.01	2	24.50	6.14	0.03534	0.6717	0.5622	Significant

Table 3 Comparison of Predicted and Experimental values for Optimised Formulation

Responses	OF5		
	Predicted	Experimental	Relative error %
Vesicle size (nm)	150.08	147.6	1.65%
Entrapment efficiency %	80.39	81.3	1.13%

Table 4 Stability studies of optimised AA loaded liposomes

Temperatures	Months	0	2	4	6
4 °C	Particle size (nm)	147.6	148	146	148.2
	EE%	81.3	79.5	80.45	79.62
25 °C	Particle size (nm)	147.6	149	150	154
	EE%	81.3	82.8	83.8	82.6
40 °C	Particle size (nm)	147.6	169	193	209
	EE%	81.3	84.6	88.4	92.1

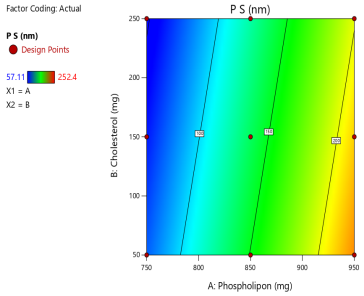

Figure 1: Contour plot for Response Y1 vesicle size.

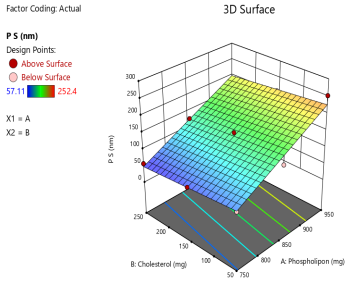

Figure 2: Response Surface Plot for Response Y1 vesicle size.

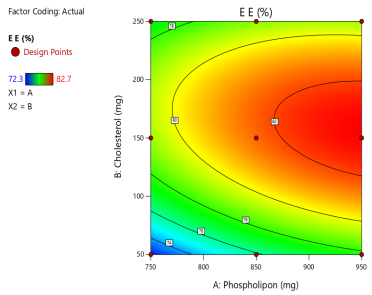

Figure: 3 Contour plot for Response Y2 Entrapment efficiency.

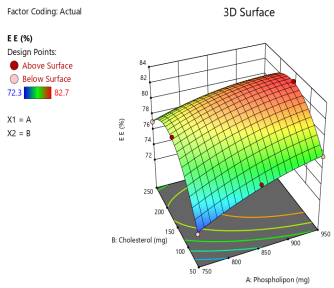

Figure 4: Response Surface Plot for Response Y2 Entrapment efficiency.

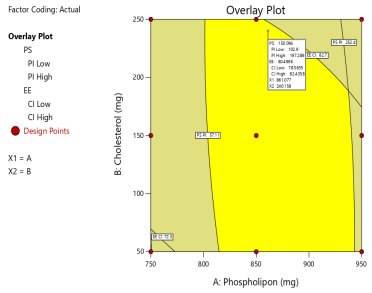

Figure 5: Overlay plot of predicted liposomal formulation.

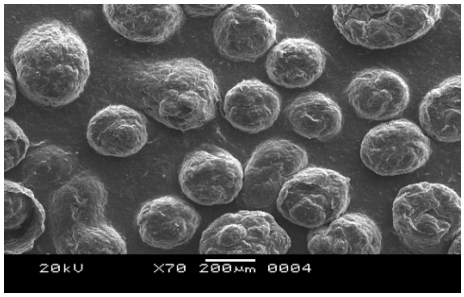

Figure 6: Scanning electron microscopic image of AAL-400 loaded liposomes.

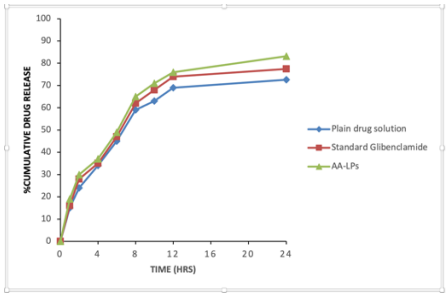

Figure 7: *In vitro* dissolution profile.

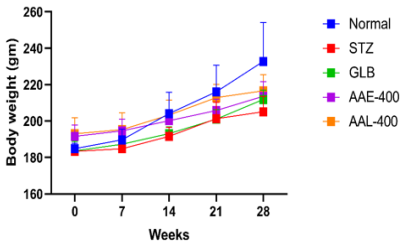

Figure 8: Effect of AAL-400 on Body weight.

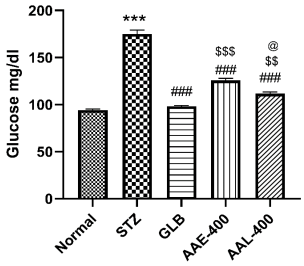

Figure 9: Effect of AAL-400 on Fasting blood glucose level.

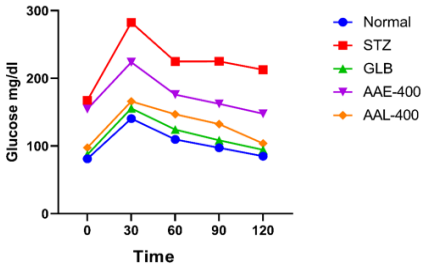

Figure 10: Effect of AAL-400 on Oral glucose tolerance test.

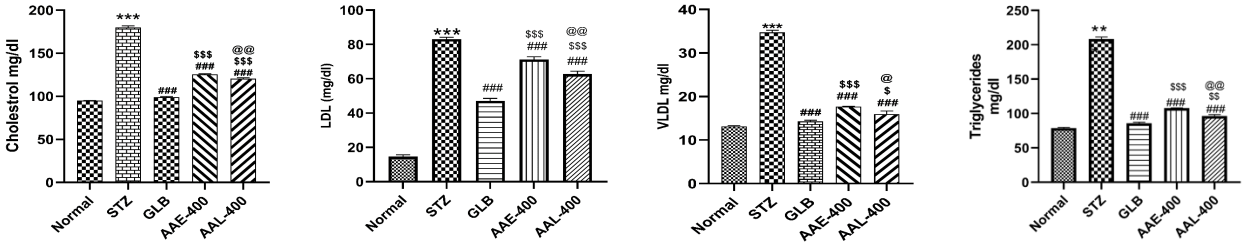

Figure 11: Effect of AAL-400 on Total cholesterol, Triglycerides, low-density lipoprotein, and very low-density lipoprotein.

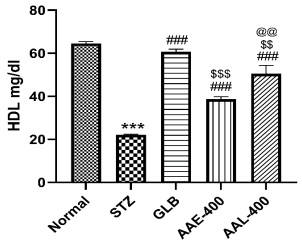

Figure 12: Effect of AAL-400 on High-density lipoprotein.

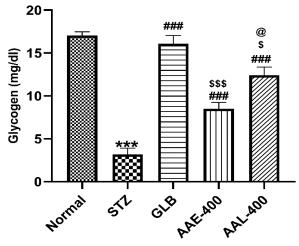

Figure 13: Effect of AAL-400 on Glycogen content in the liver.

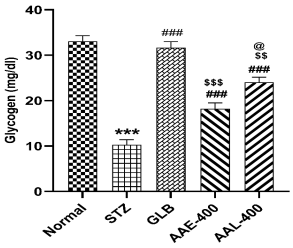

Figure 14: Effect of AAL-400 on glycogen content in skeletal muscles.

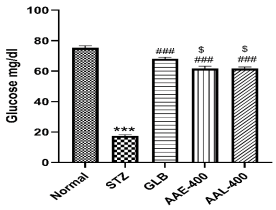

Figure 15: Effect of AAL-400 on glucose uptake in rat hemi diaphragm.

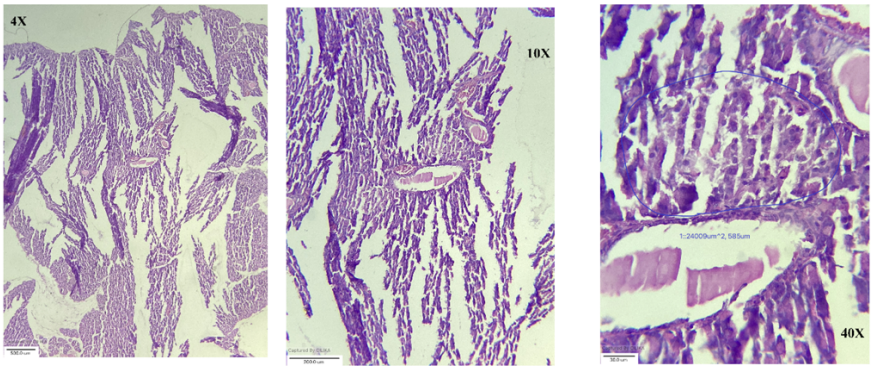

Figure 16: Effect of AAL-400 on Pancreas.

RESULTS AND DISCUSSION

Nine batches were created, one of which was optimised using Design-expert® 13.0 software based on the interactions between phospholipid and cholesterol ratios. Liposomes with vesicle sizes ranging from 57.11 nm to 252.4 nm and entrapment efficiencies ranging from 72.3% to 82.7% were obtained. Using Design Expert software, the results were fitted into various mathematical models, including linear, two-factor interaction, and quadratic models. Using multivariate linear regression analysis, quadratic terms of polynomial equations were generated for each response variable. The polynomial equation below shows how independent variables influence dependent variables.

Y = X1+X2+X1X2 equation

The sign of the coefficients in the polynomial equation represents the synergistic (denoted by the +ve sign) or antagonistic (denoted by the -ve sign) effect on responses. The predicted R2 of the model indicates how well the data fit the model. If the predicted R-squared and the adjusted R-squared are not within 0.20 of one another, there may be a problem with the data or the model. The significance of the correlation coefficient was denoted by the probability value (p 0.05). A signal-to-noise ratio indicates adequate precision by comparing the predicted value range to the average prediction error at the design points. Model discrimination is adequate when the ratio is greater than four. One-way ANOVA was used to determine the statistical significance of the model (p 0.05). The interaction between the dependent and independent variables was investigated further using contour and response surface plots. The Design Expert software generated two-dimensional contour plots based on equations and three-dimensional response surface plots. The analysis of the simultaneous effects of two factors on the response and the prediction of dependent variable responses at intermediate levels of independent variables benefit significantly from using these plots. Applying constraints (goals) to both variables (dependent and independent) resulted in an optimised formulation. The experimental data of the responses were quantitatively compared to those of the predicted values to validate the chosen experimental design, and the percent relative error was calculated.

The effect of an independent variable on AA-LP vesicle size

Table 1 shows the vesicle size of formulations. AA-LP3 had the smallest vesicle size of 57.11 nm, while AA-LP7 had the largest vesicle size of 252.4 nm. The following equation describes the effect of an independent variable on vesicle size: - Y1=137.04 + 75.36X1+5.23X2, where Y1 is vesicle size, X1 is phospholipid amount, and X2 is cholesterol amount. The equation shows that both variables positively impact vesicle size, which means that as phospholipid and cholesterol concentrations increase, so does the

vesicle size of liposomes. The high X1 coefficient indicates that the amount of phospholipid has a more pronounced effect on AA-LP vesicle size. According to the ANOVA results (Table 2), the F value for vesicle size is 36.23, with a p-value of 0.0004 indicating that the model was significant and values of 'Prob >F' indicating that all of the terms in the model are statistically significant p 0.05. The predicted R2 value of 0.9235 agrees well with the adjusted R2 value of 0.8980, indicating a good fit. Adequate precision determines the signal-to-noise ratio. As a result, the quadratic model was used to investigate the design space. The effect of changing the AA-LP vesicle size independent variable is shown in the 2D contour plot (Figure 1) and 3D response surface (Figure 2). The graphs show that increasing the amount of phospholipid from 750 mg to 950 mg increases the vesicle size of liposomes, whereas increasing the amount of cholesterol from 50 mg to 250 mg decreases the vesicle size [17, 18]. According to the previously published articles, vesicle size increases due to the presence of cholesterol in the phospholipid bilayer, resulting in larger vesicle size when hydrated above the phospholipid transition temperature. As a result, cholesterol is responsible for liposome rigidity, which makes the outer membrane phospholipid bilayer rigid, resulting in a larger vesicle size.

The increased vesicle size may be due to cholesterol accommodation in the phospholipid bilayer when hydrated above the phospholipid transition temperature, resulting in larger vesicles. Furthermore, cholesterol stiffens the phospholipid lipid bilayer membrane, resulting in larger liposomes.

Effect of an independent variable on AA-LP entrapment efficiency

Table 1 displays the entrapment efficiency of formulations. AA-LP1 had the lowest entrapment efficiency of 72.3%, while AA-LP8 had the highest entrapment efficiency of 82.7%. The following equation describes the effect of an independent variable on entrapment efficiency: - Y2=78.29 + 1.78X1+2.23X2, where Y2 is entrapment efficiency, X1 is phospholipid amount, and X2 is cholesterol amount. The equation shows that both variables positively impact entrapment efficiency, which means that as phospholipid and cholesterol concentrations increase, so does the entrapment efficiency of liposomes. The high X1 coefficient indicates that the amount of phospholipid has a greater effect on the entrapment efficiency of AA-LPs. According to the ANOVA results (Table 2), the F value for vesicle size is 6.14, with a p-value of 0.00353 indicating that the model was significant, and values of 'Prob>F' indicating that all of the terms in the model are statistically significant p0.05. The predicted R2 value of 0.671 agrees well with the adjusted R2 value of 0.5622, indicating a good fit. Adequate precision determines the signal-to-noise ratio. As a result, the quadratic model was used to investigate the design space. The effect of changing the AA-LP vesicle size independent variable is shown in the 2D contour plot (Figure 3) and 3D response surface (Figure 4). The graphs show that increasing the amount of phospholipid from 750 mg to 950 mg increases liposome entrapment efficiency while increasing the amount of cholesterol from 50 mg to 250 mg decreases entrapment efficiency [17, 18]. According to Mangesh D. *et al.,* the finding's increased drug entrapment could be attributed to bilayer membrane stabilisation and decreased entrapped drug leakage from liposomes.

The contour plots were created to predict the optimal formulation using dependent variable constraints. Table 3 and Figure 5 show an overlay plot of liposomes. The predicted formulation composition was matched with AA-LP5 liposomes that had been optimised. The experiment, however, was repeated to confirm the results. The percentage of relative error was calculated. The maximum percentage relative error found was 1.65. The values, however, were less than 5%, confirming the suitability of the experimental design used in this study [17].

SEM- Scanning Electron Microscopy

Figure 6 depicts the image of AA-LP5. SEM was used to examine the vesicle shape and morphology of the optimised formulation AA-LP5. The vesicles have an internal aqueous phase and are smooth and spherical with sharp boundaries.

***In vitro* dissolution studies**

The dissolution profile of an optimised liposome formulation, a standard drug solution, and a plain drug solution were all measured. It was done for 24 hours. Figure 7 depicts the cumulative drug percent release plotted against time. The maximum percentage of drug releases discovered was 83.2%. Compared to standard and plain extract solutions, the optimised liposome formulation AA-LP with high entrapment efficiency and small vesicle size demonstrated maximum release. The drug release of AA-LP was 83.2%, 77.5% for the standard formulation, and 72.6% for the plain extract solution. [19, 20]

Stability studies

The long-term stability ensures the dosage form's acceptability. Liposome preparations were kept in airtight amber bottles at three different temperatures: 4 2° C, 25 2° C, and 40 2° C. The most common problems encountered during liposome storage are vesicle aggregation, bilayer fusion, vesicle size increase, and drug leakage**.** Table 4 shows the results of liposome stability studies.

Liposomes were stable at 4 2°C, with no changes in vesicle size or entrapment efficiency over 6 months, whereas at 25 2°C, there were slight changes in the liposome formulations in terms of vesicle size and entrapment efficiency. Liposome preparations, on the other hand, were unstable at 40 2°C, with larger vesicle sizes that were highly aggregated towards each other and higher entrapment efficiency. Liposome formulations are thus more stable at low temperatures of 4 2°C rather than 25 2°C and 40 2°C.

Experimental pharmacology (animal study)

Effect of AAL-400 on body weight: One week after Streptozotocin and Nicotinamide injections, there was a significant decrease in body weight compared to the normal control group. Similarly, after 28 days of therapy, the AAL-400 group had significantly more body weight than the diabetic control group (P 0.001). Figure 8 shows that there was no significant difference between AAL and AAE.

Effect of AAL-400 on fasting blood glucose and OGTT: At the end of the study, fasting blood glucose levels (FBGL) in the diabetic control group were significantly higher (P 0.001) than in the normal control, a condition that was significantly reversed (P 0.001) by treatment with glibenclamide, AAE-400, and AAL-400. Figure 9 shows a significant decrease in FBGL in the AAL-400 treated group (P 0.0023) compared to the AAE-400 treated group. The OGTT was performed at 0, 30, 60, and 90 minutes intervals. Compared to the diabetic group, AAL-400 and AAE-400 showed a dose-dependent decrease in glucose levels. Figure 10 shows a significant reduction in glucose levels in the AAL-400 treated group (P = 0.0102) compared to the AAE-400 treated group.

Effect of AAL-400 on Lipid profile: there was highly significant (p 0.0001) in the diabetic group when compared to the GLB-400, AAL-400, and AAE-400 treated groups. As shown in Figure 11, there was a significant decrease (P 0.001) in total cholesterol

levels (TC), (TG), (LDL), and (VLDL) with the AAL-400 treatment compared to the AAE-400 treatment.

High-density lipoprotein (HDL) decreased significantly (p 0.0001) in the diabetic control group compared to the GLB, AAL-400, and AAE-400 treated groups. Figure 12 shows a significant increase (p0.001) in HDL in AAL-400 treated groups compared to AAE-400 groups.

Effect of AAL-400 on glycogen content in liver and skeletal muscles: there was a significant (p 0.001) in the diabetic control group when compared to the GLB, AAE-400, and AAL-400 treated groups. As shown in Figure 13, there was an increase in glycogen content in the liver for the AAL-400 treated group compared to the AAE-400 treated group.

There was a significant decrease in glycogen content in muscles for diabetic control (p 0.001) when compared to the GLB, AAE-400, and AAL-400 treated groups. As shown in Figure 14, the increase in glycogen content in skeletal muscles for AAL-400 was greater than, but not significant enough, when compared to AAE-400.

Effect of AAL-400 on the percentage of glucose uptake in rat hemi diaphragm: there was a significant (p 0.001) after 28 days in isolated rat hemi diaphragm from the diabetic control group compared to the normal control. As shown in Figure 15, there was no significant difference in glucose uptake in the rat hemi diaphragm between the AAL-400 and AAE-400 groups.

Histology of pancreas: The diabetic control group had a significant decrease in the average size and number of pancreatic cells compared to the normal group. GLB, AAE-400, and AAL-400 treatments reversed this condition. AAL-400 also had better histological findings than AAE-400, with less venous congestion, as shown in Figure 16**.**

CONCLUSION

Phenolic phytoconstituents such as flavonoids have been reported for various biological activities such as antidiabetic effect; however, many *in silico*, *in vitro*, and *in vivo* studies for various flavonoid-loaded liposome systems to enhance its solubility and stability have been reported. However, in terms of efficiency, the optimisation of formulations through a design expert approach will aid in utilising and optimising herbal Nano drug delivery systems for improved therapeutic activity.

ACKNOWLEDGMENT

The authors thank Principal Maratha Mandal's College of Pharmacy, Belagavi, for his constant support.

REFERENCES

1. Ahmad E, Sargeant JA, Yates T, Webb DR, Davies MJ. Type 2 Diabetes and Impaired Physical Function: A Growing Problem. Diabetol. 2022:11;3(1):30-45.
2. Elosta A, Ghous T, Ahmed N. Natural products as anti-glycation agents: possible therapeutic potential for diabetic complications. Curr. Diabetes Rev. 2012:1;8(2):92-108.
3. Arroba AI, Aguilar-Diosdado M. Special Issue "The Prevention, Treatment, and Complications of Diabetes Mellitus". J. Clin Med. 2022;9;11(18):5305.
4. Babu D, Kumar P. Effect of Polyherbal Formulation in Patients with Type 2 Diabetes Mellitus Journal Med Sci & Tech. 2013:2(1); 22.
5. Zhou Y, Underhill SJ. Characterisation of Breadfruit (*Artocarpus altilis*) Plants Growing on Lakoocha (*A. lakoocha*) Rootstocks. Horticulture. 2022:7;8(10):916.
6. Mohanty M, Pradhan C. A review on phytochemistry, bio-efficacy, medicinal and ethno-pharmaceutical importance of *Artocarpus altilis*. Int. J. Pharm. Pharm. Res. 2015;3:219-31.
7. Sikarwar MS, Hui BJ, Subramaniam K, Valeisamy BD, Yean LK, *et al*. A review on *Artocarpus altilis* (Parkinson) Fosberg (breadfruit). J. Appl Pharm. Sci. 2014: 27;4(8):091-7.
8. Tamègnon AK, Innocent YB, Célestin TC, Roseline B, Pivot SS, *et al*. Uses of the fruit of breadfruit tree (*Artocarpus altilis*) in the Republic of Benin: Bibliographic Synthesis. Intl J Agron Agric Res. 2017;11:69-81.
9. Fricker G, Kromp T, Wendel A, Blume A, Zirkel J, *et al*. Phospholipids, and lipid-based formulations in oral drug delivery. Pharm. Res. 2010:27(8):1469-86.
10. Mishra H, Chauhan V, Kumar K, Teotia D. A comprehensive review on Liposomes: a novel drug delivery system. J. drug deliv. Ther. 2018: 25;8(6):400-4.
11. Andra VV, Bhatraju LV, Ruddaraju LK. A comprehensive review on novel liposomal methodologies, commercial formulations, clinical trials and patents. BioNanoScience. 2022:26:1-8.
12. Amin SG, Shah DA, Dave RH. Formulation and evaluation of liposomes of fenofibrate prepared by thin film hydration technique. Int. J. Pharm. Sci. Res. 2018: 1;9(9):3621-7.
13. Tawfeek HM, Abdellatif AA, Abdel-Aleem JA, Hassan YA, Fathalla D. Transfersomal gel nanocarriers for enhancement the permeation of lornoxicam. J. Drug Deliv Sci Technol. 2020: 1;56:101540.
14. Dudhipala N, Phasha Mohammed R, Adel Ali Youssef A, Banala N. Effect of lipid and edge activator concentration on development of aceclofenac-loaded transfersomes gel for transdermal application: *In vitro* and *ex vivo* skin permeation. Drug Dev Ind Pharm. 2020: 2;46(8):1334-44.
15. Lujan H, Griffin WC, Taube JH, Sayes CM. Synthesis and characterisation of nanometer-sized liposomes for encapsulation and microRNA transfer to breast cancer cells. Int J Nanomedicine. 2019;14:5159.
16. Godbole MD, Sabale PM, Mathur VB. Development of lamivudine liposomes by three-level factorial design approach for optimum entrapment and enhancing tissue targeting. J. Microencapsul. 2020: 17;37(6):431-44.
17. Sudhakar B, Krishna MC, Murthy KV. Factorial design studies of antiretroviral drug-loaded stealth liposomal injectable: PEGylation, lyophilisation and pharmacokinetic studies. Appl. Nanosci. 2016:6(1):43-60.
18. Peram MR, Jalalpure S, Kumbar V, Patil S, Joshi S, *et al*. Factorial design-based curcumin ethosomal nanocarriers for the skin cancer delivery: *in vitro* evaluation. J. liposome Res. 2019:3;29(3):291-311.
19. Rathod S, Deshpande SG. Design and evaluation of liposomal formulation of pilocarpine nitrate. Indian J. Pharm. Sci. 2010: 72(2):155.
20. Purushotham M, Viswanath V, Narashimha Rao B, Irshad Begam S. Preparation, and evaluation of Decitabine liposomes, Indo Am. J. Pharm. Sci. 2015:27; 2(9), 1264-1273.
21. Muppidi K, Pumerantz AS, Wang J, Betageri G. Development and stability studies of novel liposomal vancomycin formulations. Int. Sch. Res. Notices. 2012.
22. Masiello P, Broca C, Gross R, Roye M, Manteghetti M, *et al*. Experimental NIDDM: development of a new model in adult rats administered streptozotocin and nicotinamide. Diabetes. 1998:1;47(2):224-9.
23. Kumar R, Patel DK, Prasad SK, Sairam K, Hemalatha S. Antidiabetic activity of alcoholic root extract of *Caesalpinia*

digyna in streptozotocin-nicotinamide induced diabetic rats. Asian Pac. J. Trop. Biomed. 2012:1;2(2):S934-40.
24. Seifter S, Dayton S, Novic B, Muntwyler E. The estimation of glycogen with the anthrone reagent. Arch. Biochem. 1950; 25:191-200.

Cite this article as:

Archana M. Patil, Sarvanan Kaliyaperumal and Mrityunjaya B. Patil. Formulation, optimisation and characterisation of *Artocarpus altilis* loaded liposomes for antidiabetic activity. Int. J. Res. Ayurveda Pharm. 2023;14(2):91-98
DOI: http://dx.doi.org/10.7897/2277-4343.140248

Source of support: Nil, Conflict of interest: None Declared